

# Activation of the Notch signaling pathway in the anterior cingulate cortex is involved in the pathological process of neuropathic pain

Haifeng Duan<sup>a</sup>, Fengyan Shen<sup>a</sup>, Li Li<sup>a</sup>, Zhiyi Tu<sup>b</sup>, Ping Chen<sup>a</sup>, Pei Chen<sup>b</sup>, Zhiru Wang<sup>c</sup>, Weimin Liang<sup>a</sup>, Yingwei Wang<sup>a,\*</sup>

## Abstract

Plastic changes in the anterior cingulate cortex (ACC) are critical in pain hypersensitivity caused by peripheral nerves injury. The Notch signaling pathway has been shown to regulate synaptic differentiation and transmission. Therefore, this study was to investigate the function of the Notch signaling pathway in the ACC during nociceptive transmission induced by neuropathic pain. We adopted Western blotting, N-[N-(3,5-difluorophenacetyl)-l-alanyl]-S-phenylglycine t-butyl ester (DAPT) microinjections, RNA interference targeting Notch1, Hairy and enhancer of split (Hes) 1 or Hes5, electrophysiological recordings, and behavioral tests to verify the link between Notch signaling in ACC and neuropathic pain with adult male Sprague-Dawley rats. Levels of the Notch intracellular domain were increased in ACC on day 7 after chronic constriction injury surgery or spared nerve injury. Meanwhile, the mRNA level of the downstream effector of Notch signaling Hes1 was increased, whereas the level of Hes5 mRNA did not change. Microinjection of DAPT, a  $\gamma$ -secretase (a key enzyme involved in Notch pathway) inhibitor, into ACC significantly reversed neuropathic pain behaviors. Intra-ACC injection of short hairpin RNA-Notch reduced Notch intracellular domain expression and decreased the potentiation of synaptic transmission in the ACC. Moreover, pain perceptions were also alleviated in rats subjected to chronic constriction injury or spared nerve injury. This process was mainly mediated by the downstream effector Hes1, but not Hes5. Based on these results, the activation of the Notch/Hes1 signaling pathway in the ACC participates in the development of neuropathic pain, indicating that the Notch pathway may be a new therapeutic target for treating chronic pain.

**Keywords:** Neuropathic pain, Notch signaling pathway, Anterior cingulate cortex, Synaptic transmission, Central sensitization

## 1. Introduction

Neuropathic pain is one of the most debilitating types of pain and affects approximately 8% of the global population, despite the availability of a variety of treatment options. It is an important public health problem caused by a lesion or disease in the somatosensory nervous system, and is characterized by spontaneous pain, thermal hyperalgesia, and mechanical allodynia.<sup>6,19,38</sup> Pain is one of the most common clinical symptoms. Once it tends to be chronic, it will produce a series of pathological

changes to the organism, and pain itself has become a disease. Neuropathic pain is a typical example. Strangely, classic analgesics have limited therapeutic effect on neuropathic pain, whereas the antidepressants and anticonvulsants show certain effects at low doses.<sup>40</sup> Thus, the elucidation of the underlying mechanisms of neuropathic pain and development of new therapeutic agents are major challenges.

The mechanisms of neuropathic pain are complicated due to the presence of many factors. Central sensitization is considered to play an important role in the mechanism of neuropathic pain. The anterior cingulate cortex (ACC) is a structure in the limbic system that is responsible for the emotional processing of noxious stimuli.<sup>20,23,33</sup> It is a complex and heterogeneous cortical region that mainly receives afferent inputs from the medial thalamic nuclei containing nociceptive neurons that receive input from the spinothalamic tract.<sup>10,36</sup> However, neurons in the ACC have recently been shown to play pivotal roles in mediating the somatosensory component of physiological and pathological pain. Disruption of long-term potentiation in the ACC relieves neuropathic pain<sup>33</sup> and a local lesion or electrical stimulation effectively reduces neuropathic pain in both human and rats.<sup>31,44</sup> Those findings have prompted particular interest in the ACC as a region involved in the neural mechanism of neuropathic pain.

The Notch signaling pathway is a highly conserved pathway throughout evolution. It originated from genetic studies in *Drosophila*, when observed in mutant flies with notched wings, a phenotype that later provided the name for it. Notch is a transmembrane signaling protein. Interaction of the receptor with

Sponsorships or competing interests that may be relevant to content are disclosed at the end of this article.

H. Duan, F. Shen, and L. Li contributed equally to this work.

<sup>a</sup> Department of Anesthesiology, Huashan Hospital, Fudan University, Shanghai, China, <sup>b</sup> Department of Anesthesiology, Shanghai Tenth People's Hospital, Tongji University School of Medicine, Shanghai, China, <sup>c</sup> Key Laboratory of Brain Functional Genomics-Ministry of Education, School of Life Science, East China Normal University, Shanghai, China

\*Corresponding author. Address: Department of Anesthesiology, Huashan Hospital, Fudan University, Shanghai 200040, China. Tel.: +86-21-5288-7689. E-mail address: wangyw@fudan.edu.cn (Y. Wang).

PAIN 162 (2021) 263–274

Copyright © 2020 The Author(s). Published by Wolters Kluwer Health, Inc. on behalf of the International Association for the Study of Pain. This is an open access article distributed under the terms of the Creative Commons Attribution-Non Commercial-No Derivatives License 4.0 (CCBY-NC-ND), where it is permissible to download and share the work provided it is properly cited. The work cannot be changed in any way or used commercially without permission from the journal.

<http://dx.doi.org/10.1097/j.pain.0000000000002014>

a transmembrane ligand on a juxtaposed cell results in proteolytic cleavage of the receptor, first by an ADAM metalloprotease and subsequently by the  $\gamma$ -secretase enzyme complex. The latter cleavage liberates the Notch intracellular domain (NICD) that translocates to the cell nucleus, where it regulates the transcription of downstream genes.<sup>32</sup> Notch signaling plays important roles in many physiological and pathological developmental processes such as vasculogenesis, cell proliferation and migration, immune response, cancer metastasis, and memory and neurological diseases.<sup>25,28,41</sup>

Activation of Notch signaling regulates synaptic differentiation and transmission in the hippocampus.<sup>1,5</sup> Moreover, the Notch pathway plays a pivotal role in the induction and maintenance of neuropathic pain at the spinal level.<sup>37</sup> Researchers have not clearly determined whether the Notch signaling pathway plays a role in central sensitization in ACC induced by neuropathic pain. Therefore, this study intended to illustrate the effect of the Notch signaling pathway on neuropathic pain in the ACC of animal models with peripheral nerve injury.

## 2. Materials and methods

### 2.1. Experimental animals

Adult male Sprague-Dawley rats weighing 240 to 340 g and aged 9 to 11 weeks (Shanghai Sipper; BK Laboratory Animals Co, Ltd, Shanghai, China) were maintained at a room temperature of 23 to 28°C and at 50% to 60% humidity on a 12-hour light/dark cycle with free access to water and food. Efforts were made to reduce the number of animals used to the minimum number required for statistical accuracy and minimize their suffering. The animals were anesthetized with an intraperitoneal injection of pentobarbital sodium (40 mg/kg) when surgical procedures were performed. The procedures adhered to the National Institutes of Health Guide for the Care and Use of Laboratory Animals and were approved by the Ethical Committee for Animal Research of Fudan University (No. 201802130S).

### 2.2. Chronic constriction injury surgery

Chronic constriction injury (CCI) surgery was performed in accordance with the method described in a previous study<sup>3</sup> and followed the ethical guidelines of the International Association for the Study of Pain regarding the use of laboratory animals. Animals were randomly allocated to each group and then intraperitoneally injected with pentobarbital sodium before surgery. In the CCI group, the left sciatic nerve of rats was exposed unilaterally at the midhigh level, and 4 chromic gut (5-0) ligatures were tied loosely around the nerve proximal to its trifurcation at 1 to 1.5 mm intervals. The sciatic nerve was exposed without ligation for the sham surgery. The day of surgery was considered day 0. After CCI, the rats walked with an obvious limp, raised the affected hind paw, and held it in a protected position with the toes together,<sup>3</sup> which was not observed in other rats.

### 2.3. Spared nerve injury surgery

The spared nerve injury (SNI) model was established as previously described.<sup>12</sup> Briefly, an incision was made on the upper edge of the left hind leg of the rat. The muscles were separated to expose the sciatic nerve trunk and carefully separate its 3 branches: tibial, common peroneal, and sural nerves. Then, the tibial and peroneal nerves were ligated and 2 to 3 mm of the nerves distal to the ligation was removed, whereas the sural nerve remained intact. Then, the

muscle and skin incisions were closed. In the sham surgery groups, only the sciatic nerve trunk and its branches were exposed, but the animals did not undergo ligation and transection.

### 2.4. Cannulation and microinjection

The rats were anesthetized with pentobarbital sodium and fixed on a stereotaxic apparatus with the bregma and lambda at the same horizontal level. A 30-gauge stainless steel guide cannula with a 33-gauge stainless steel stylet plug (Shenzhen RWD Life Science Co, Ltd, Shenzhen, China) was bilaterally implanted into the ACC (2.7 mm anterior from the bregma,  $\pm$  0.6 mm lateral to the midline, and 2.0 mm ventral from the dura; 0.4 mm anterior from the bregma,  $\pm$  0.6 mm lateral to the midline, and 2.0 mm ventral from the dura) according to the rat brain atlas. Next, 3 stainless steel screws were inserted into the skull around the cannulas and fixed with dental acrylic. The dummy cannulas were left in place for the infusion. After cannulation, animals were housed individually. For infection prophylaxis, penicillin (80,000 units) was administered 1 day before surgery and 2 consecutive days after surgery. The cerebral microinjection was performed one week after cannulation. Before the microinjection, the dummy cannulas were removed and internal injection cannulas (32 gauge), which extended 0.5 mm beyond the guide cannulas, were inserted. A 10- $\mu$ L Hamilton syringe was connected to the injection cannula by a long flexible pipe and driven by an automated syringe pump (Stoelting Co., Wood Dale, IL). A volume of 2  $\mu$ L of solution was injected at a rate of 0.2  $\mu$ L/minute. The injection cannula was left in place for additional 5 minutes to minimize the efflux of the drug. Animals were allowed additional 1 hour to recover before beginning the behavior tests. DAPT was microinjected into the bilateral ACC region of the brain once daily on days 0, 1, 2, 3, and 4 after CCI. For the microinjection, N-[N-(3,5-difluorophenacetyl)-l-alanyl]-S-phenylglycine t-butyl ester (DAPT, 5 mg; Sigma-Aldrich China, Catalog #D5942, Shanghai, China) was dissolved in a solution of dimethyl sulfoxide prepared in 0.1M sterile phosphate-buffered saline (PBS) that was ultrasonicated for 10 minutes. Vehicle-treated animals received similar volumes of 0.1M sterile PBS or 0.1M sterile PBS with 1% dimethyl sulfoxide.

### 2.5. Mechanical allodynia test

The mechanical threshold of the ipsilateral hind paws of the rats was tested, and the experimenter was blinded to the drug application. All rats were placed in a Plexiglas box with a metal net bottom for 30 minutes per day for 3 days before the tests. After habituation to the environment, a series of von Frey hairs with logarithmically increasing stiffness (0.4, 1, 1.4, 2, 4, 6, 8, 10, and 15 g) (Stoelting Co) were used to stimulate the hind paw. The filament was applied perpendicular to the plantar surface with a sufficient force to bend it for 3 seconds. A positive performance was recorded if the hind paw was rapidly lifted and completely raised from the platform. We used the up-down method to determine the withdrawal threshold.<sup>7</sup>

### 2.6. Thermal hyperalgesia test

Thermal hyperalgesia was assessed using the test described by Hargreaves et al.<sup>15</sup> After habituation in the Plexiglas box on a 3-mm-thick glass plate for 30 minutes, the plantar surface of the hind paw of each animal was irradiated with heat source within a 0.5-cm-diameter circle using a BME-410 thermal radiation stimulator (Institute of Biomedical Engineering, Peking Union Medical College, Tianjin, China) at 10 V and 30 W. The time from

the start of irradiation to paw withdrawal was considered the paw withdrawal latency value to reflect the threshold of thermal sensitivity. Thirty seconds was set as the cutoff time to avoid tissue injury. Each hind paw was tested 3 times with a 6- to 8-minute interval between trials, and the mean value was calculated for the analysis.

### 2.7. Open-field test

The open-field test was applied to detect movement. All animals were acclimated to the testing room for 30 minutes before the test. The rats were individually placed at the center of the box, which had 4 transparent walls, a gray bottom, and an open top. The total distance that each rat traveled in 15 minutes was measured with a tracking analysis system (Coulbourn Instruments, Holliston, MA). The distance was used as a parameter for rat locomotion.

### 2.8. Adeno-associated virus generation and injection

A short hairpin RNA (shRNA) targeting Notch1 was constructed and inserted in an adeno-associated virus (AAV) vector carrying a green fluorescent protein (GFP) by Obio Technology (Shanghai, China); this shRNA specifically targets rat neurons and enables significant downregulation of Notch1 expression. In addition, shRNAs targeting Hes1 and Hes5 were constructed to downregulate the expression of Hes1 and Hes5, respectively. Briefly, the coding sequences of the genes were artificially synthesized. The same vector backbone was used to generate a negative control.

For the virus microinjection, rats were anesthetized by administering an intraperitoneal injection of sodium pentobarbital and placed in a stereotactic frame. Then, the rats were injected with 2  $\mu$ L of the virus or DAPT into the bilateral ACC with a microsyringe (10  $\mu$ L) at a slow rate (over 5 minutes). The microsyringe was left in place for additional 5 minutes and slowly withdrawn to prevent back flow.

### 2.9. Reverse transcription-quantitative polymerase chain reaction

Total RNAs were extracted from the ACC using a High Pure RNA Tissue Kit (Roche) according to the manufacturer's instructions. Real-time quantitative PCR was performed to analyze levels of the Notch1, Hes1, and Hes5 transcripts using a StepOne Real-Time PCR System (ABI). Primers for the selected genes were designed using Primer 5.0 software (Premier, Palo Alto, CA), and their specificity was confirmed by a BLAST search (<http://www.ncbi.nlm.nih.gov/blast/Blast.cgi>). GAPDH served as an endogenous control gene. Primers were purchased from Invitrogen. The following primers were used for qRT-PCR: Notch1: Forward 5-TGCCAACA-TCCAAGACAAC-3, Reverse 5-CATCCACAGCATTGACATCAG-3, length of the amplified product, 218 bp; Hes1: Forward 5-GAAAGATAGCTCCCGGCATTCC-3, Reverse 5-CTCGTTCAT-GCACTCGCTGAAG-3, length of the amplified product, 163 bp; Hes5: Forward 5-GCTGAACTGCTGCTGGAG-3, Reverse 5-GCCGCTGGAAGTGGTAAAG-3, length of the amplified product, 251 bp; and GAPDH: Forward 5-GGAGTCTACTGGCGTCTTCAC-3, Reverse 5-ATGAGCCCTTCCACGATGC-3, length of the amplified product, 237 bp.

### 2.10. Western blot

The rats were deeply anesthetized with an i.p. injection of sodium pentobarbital, decapitated, and then the regions encompassing the bilateral ACC and hippocampus were dissected at designated time

points and preserved in liquid nitrogen. Next, total proteins were extracted from the ACC and hippocampus by homogenizing the tissues in ice-cold RIPA lysis buffer (Beyotime Biotechnology, Shanghai, China) supplemented with 0.1 mM phenylmethylsulfonyl fluoride-protease inhibitors and phosphatase inhibitors, lysed on ice for 30 minutes, and centrifuged at 4°C for 10 minutes. Samples were heated at 95°C for 10 minutes in loading buffer before equal amounts of protein were loaded onto a 10% sodium dodecyl sulfate-polyacrylamide gel electrophoresis (SDS-PAGE), electrophoretically separated, and then transferred to polyvinylidene difluoride membranes at 4°C. After blocking with 5% nonfat milk for 2 hours at room temperature, membranes were incubated overnight at 4°C with a primary antibody against NICD (1:1000 dilution; Cell Signaling Technology #3608, Danvers, MA) or  $\beta$ -actin (1:500 dilution, Boster #BM3873, Wuhan, China). Membranes were washed with PBS buffer, incubated with horseradish peroxidase-conjugated secondary anti-rabbit IgG (1:2000 dilution; Abcam #ab6721, Cambridge, MA) for 2 hours at room temperature, and the bands were visualized using enhanced chemiluminescence (ECL, Thermo Fisher China, Shanghai, China). The relative levels of the target protein normalized to  $\beta$ -actin levels were determined by performing a densitometry analysis using ImageJ software (National Institutes of Health, Bethesda, MD).

### 2.11. Immunohistochemistry

We deeply anesthetized the animals with pentobarbital sodium and immediately transcardially perfused them with 0.1 M PBS (pH 7.2-7.4) followed by 4% paraformaldehyde. Then, the brains were removed and postfixed with 4% paraformaldehyde for 4 hours, followed by an incubation in 30% sucrose overnight at 4°C for cryoprotection until the tissues sank to the bottom. Sagittal sections through the entire brain were cryosectioned at a 40- $\mu$ m thickness. Then, the sections were blocked with 5% goat serum for 1 hour at room temperature and subsequently incubated overnight at 4°C with a chicken anti-GFP antibody (1:500 dilution, Abcam #ab13970). After 3 washes with PBS, sections were incubated at room temperature for 2 hours with a mixture containing 1:250 dilutions of Alexa Fluor 488-conjugated goat anti-chicken antibodies (1:1000 dilution, Abcam #ab150173). Staining of the sections was visualized with a confocal microscope.

### 2.12. Electrophysiology

The rats were deeply anesthetized and decapitated. Brains were rapidly removed and incubated in a chilled artificial cerebrospinal fluid (ACSF: 124 mM NaCl, 2.5 mM KCl, 1 mM MgSO<sub>4</sub>, 2 mM CaCl<sub>2</sub>, 1 mM NaH<sub>2</sub>PO<sub>4</sub>, 25 mM NaHCO<sub>3</sub>, and 10 mM glucose) bubbled with 95% O<sub>2</sub> + 5% CO<sub>2</sub>. The slices (400  $\mu$ m) were cut with a vibrating microtome (VT-1200; Leica Biosystems China, Shanghai, China). Slices containing the ACC were transferred to another gas interface-type recording chamber and maintained in room temperature (23  $\pm$  2°C) for at least 2 hours before the recordings.

Voltage clamp recordings were obtained from pyramidal neurons in layer II/III of the ACC slices. Whole-cell patch microelectrodes (5-7 M $\Omega$ ) were filled with (in mM) 2 MgCl<sub>2</sub>, 2 K<sub>2</sub>ATP, 1 CaCl<sub>2</sub>, 140 K-gluconate, 11 EGTA, and 10 HEPES. For the recordings of miniature excitatory postsynaptic currents (mEPSCs), tetrodotoxin (0.5  $\mu$ M) and picrotoxin (100  $\mu$ M) were present in the ACSF. An Axon 700B patch clamp amplifier (Molecular Devices, San Jose, CA) was used for the recordings. Currents were filtered at 5 kHz using a Digidata 1440 attached to Clampfit 10.1 (Molecular Devices). Recordings with steady series resistances of <30 M $\Omega$  were the only recordings included in the analysis. The series resistance and junction potential were compensated using the bridge circuit.

### 2.13. Statistical analysis

Data were analyzed with SPSS 20.0 software (SPSS Inc, Chicago, IL). The data are reported as mean  $\pm$  SEM. Student *t*-test was used when only 2 groups were compared, and one-way analysis of variance (ANOVA) with Tukey multiple-comparison post hoc tests were used when more than 2 groups of data were compared. Behavioral data were analyzed using a two-way repeated-measures ANOVA with the group as a between-groups factor and time as a repeated-measures factor, followed by the

Bonferroni post hoc test. *P* values less than 0.05 were considered statistically significant.

## 3. Results

### 3.1. Chronic constriction injury increased Notch intracellular domain levels in the anterior cingulate cortex

After the establishment of the CCI model, both mechanical allodynia and thermal hyperalgesia were produced persistently as

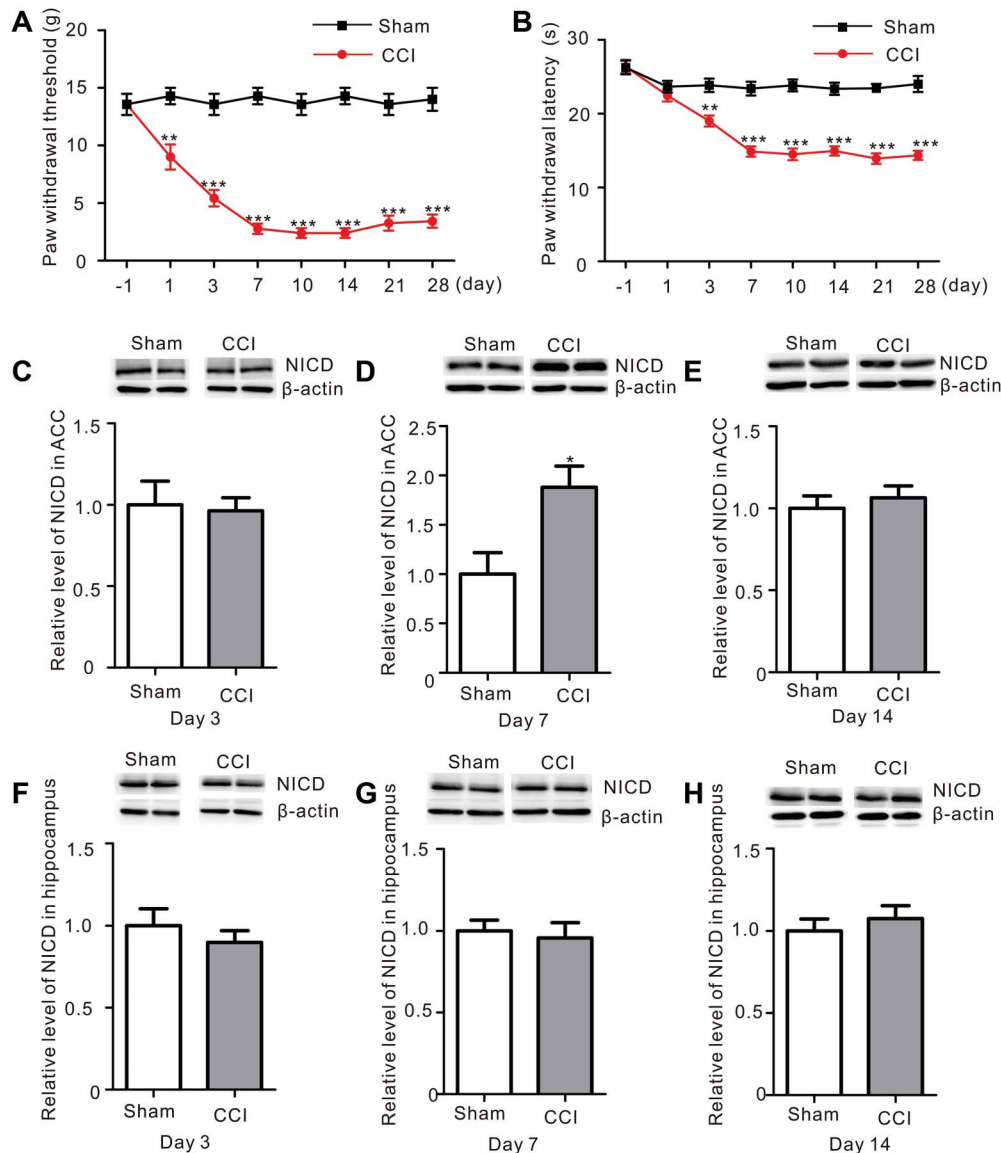


**Figure 1.** Nerve injury increases NICD levels in the ACC. (A) The two-way repeated-measures ANOVA revealed a significant effect of the interaction of surgery (Sham vs CCI) and time (day  $-1$ , 1, 3, 7, 10, 14, 21, and 28) on the mechanical withdrawal thresholds of rats ( $F = 13.76$ ,  $P < 0.001^{***}$ ,  $n = 8$  animals per group, two-way ANOVA). A post hoc test (Bonferroni) revealed a decrease in the mechanical withdrawal thresholds of the CCI compared to the Sham rats on day 1, 3, 7, 10, 14, 21, and 28 (black: Sham, red: CCI). (B) Two-way repeated-measures ANOVA revealed a significant effect of the interaction of surgery (Sham vs CCI) and time (day  $-1$ , 1, 3, 7, 10, 14, 21, and 28) on the paw withdrawal latency of rats ( $F = 12.03$ ,  $P < 0.001^{***}$ ,  $n = 8$  animals per group, two-way ANOVA). A post hoc test (Bonferroni) showed a decrease in the paw withdrawal latency in the CCI group compared to the Sham rats on days 1, 3, 7, 10, 14, 21, and 28 (black: Sham, red: CCI). (C–E) Western blot showing the levels of NICD in the ACC of Sham and CCI rats. Bottom panel, quantification of the intensity of the NICD bands (white: Sham group; gray: CCI group). NICD levels were only increased in the ACC at 7 days after CCI. The data are presented as mean  $\pm$  SEM ( $P = 0.014^*$ , Student *t*-test,  $n = 8$  samples per group). On day 3 (C) and 14 (E), no difference in the NICD levels was observed. (F–H) Western blot showing NICD levels in the hippocampus of Sham and CCI rats on day 3 (F), 7 (G), and 14 (H) after surgery. Bottom panel, quantification of the intensity of the NICD bands. A difference in NICD levels in the hippocampus was not observed at different time points (Student *t*-test,  $n = 8$  samples per group). ACC, anterior cingulate cortex; ANOVA, analysis of variance; CCI, chronic constriction injury; NICD, Notch intracellular domain.

previously reported<sup>12</sup> ([Fig. 1A, sham vs CCI,  $P < 0.001$ , two-way ANOVA], [Fig. 1B, sham vs CCI,  $P < 0.001$ , two-way ANOVA],  $n = 8$ ). The ACC is an important region of the brain involved in neuropathic pain formation.<sup>47</sup> We first examined the levels of the NICD in the ACC of rats with a peripheral nerve injury using Western blotting to explore whether the Notch signaling pathway is involved in pathologic process of neuropathic pain. Notch intracellular domain levels increased on day 7 after CCI surgery, whereas no differences were observed on days 3 or 14 (Fig. 1C, [Fig. 1D, sham vs CCI,  $P = 0.014$ , Student  $t$ -test], Fig. 1E,  $n = 8$ ).

We also examined the NICD levels in the hippocampus to investigate whether the changes were specific to the ACC. Notch intracellular domain levels in the hippocampus did not change significantly (Figs. 1F–H). Thus, CCI temporarily increased NICD levels in the ACC.

### 3.2. Microinjections of DAPT attenuated neuropathic pain

Next, we sought to assess whether Notch upregulation contributed to the pathological process of neuropathic pain.

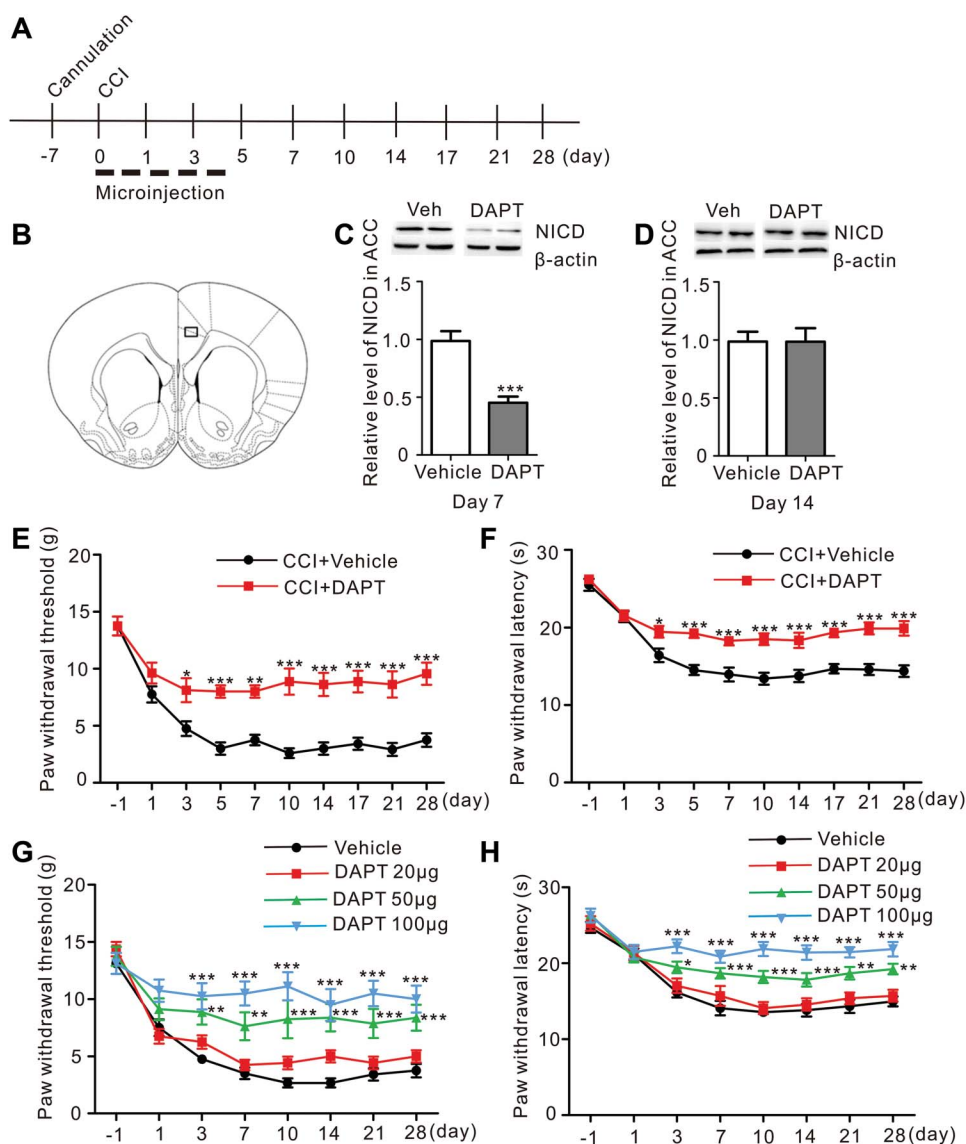


**Figure 2.** Microinjections of DAPT into the ACC relieved CCI-induced neuropathic pain in a dose-dependent manner. (A) Schematic of the early ACC microinjection experiments. (B) Representative rat section through the ACC, 1.7 mm rostral to the bregma. (C) The NICD level was significantly decreased 7 days after CCI in the DAPT group compared to the Vehicle group ( $P < 0.001^{***}$ , Student  $t$ -test,  $n = 8$  samples per group). (D) There were no differences in NICD level between DAPT and Vehicle groups 14 days after CCI. (E) Two-way repeated-measures ANOVA indicated a significant effect of the interaction of DAPT (CCI + DAPT vs CCI + Vehicle) and time (day  $-1$  to 28) on the mechanical allodynia induced by the intra-ACC microinjection of DAPT ( $F = 3.926$ ,  $P < 0.001^{***}$ ,  $n = 8$  animals per group, two-way ANOVA). A post hoc test (Bonferroni) revealed that the microinjection of DAPT reversed the mechanical allodynia of CCI rats compared to the Vehicle (black: CCI + Vehicle, red: CCI + DAPT). (F) Attenuation of CCI-induced thermal hyperalgesia by the intra-ACC microinjection of DAPT ( $F = 3.536$ ,  $P = 0.0018^{**}$ ,  $n = 8$  animals per group, two-way ANOVA followed by the Bonferroni post hoc test, black: CCI + Vehicle, red: CCI + DAPT). (G) Reversal of mechanical allodynia after CCI by microinjections of different doses of DAPT; only 50  $\mu\text{g}$  and 100  $\mu\text{g}$  significantly reversed the paw withdrawal threshold ( $F = 2.098$ ,  $P = 0.0044^{**}$ ,  $n = 8$  animals per group, two-way ANOVA followed by the Bonferroni post hoc test, black: CCI + Vehicle, red: CCI + DAPT 20  $\mu\text{g}$ , green: CCI + DAPT 50  $\mu\text{g}$ , blue: CCI + DAPT 100  $\mu\text{g}$ ). (H) Microinjections of different doses of DAPT into the ACC increased the paw withdrawal latency ( $F = 2.875$ ,  $P < 0.0001^{***}$ ,  $n = 8$  animals per group, two-way ANOVA followed by the Bonferroni post hoc test, black: CCI + Vehicle, red: CCI + DAPT 20  $\mu\text{g}$ , green: CCI + DAPT 50  $\mu\text{g}$ , blue: CCI + DAPT 100  $\mu\text{g}$ ). ACC, anterior cingulate cortex; ANOVA, analysis of variance; CCI, chronic constriction injury; DAPT, N-[N-(3,5-difluorophenacetyl)-l-alanyl]-S-phenylglycine t-butyl ester; NICD, Notch intracellular domain.

DAPT (50  $\mu$ g), a  $\gamma$ -secretase (a key enzyme involved in the Notch signaling pathway) inhibitor, was microinjected into the ACC for 5 consecutive days immediately after CCI surgery to inhibit the activation of the Notch signaling pathway (Figs. 2A and B). As a result, NICD levels were significantly decreased 7 days after the first microinjection and returned to normal on day 14 ([Fig. 2C, CCI + vehicle vs CCI + DAPT,  $P < 0.001$ , Student  $t$ -test], Fig. 2D,  $n = 8$ ). Mechanical allodynia and thermal hyperalgesia were persistently attenuated after the microinjection of DAPT (Figs. 2E and F). Moreover, DAPT microinjections exerted dose-dependent effects on neuropathic pain (Figs. 2G and H).

When DAPT was injected into the ACC 2 weeks after CCI surgery for 5 consecutive days (Fig. 3A), NICD levels also decreased (Fig. 3B, CCI + vehicle vs CCI + DAPT,  $P < 0.001$ , Student  $t$ -test,  $n = 8$ ). However, this treatment reversed mechanical allodynia and thermal hyperalgesia for only a few days (Figs. 3C and D). Then, we performed an open-field test to exclude the possible effect of DAPT on the motor functions of the rats that might alter the pain behaviors. The microinjections of DAPT for 5 consecutive days did not change the total and center distance traveled or the total and center time in the normal rats during the 30-min recording time (Figs. 3E and F). Based on these results, Notch activation might contribute to the formation of neuropathic pain.

### 3.3. Downregulating Notch1 in the anterior cingulate cortex persistently alleviated neuropathic pain

Because the  $\gamma$ -secretase complex hydrolyzes the transmembrane domains of several integral membrane proteins, including the key signaling molecule amyloid precursor protein, Notch, deleted in colorectal cancer, and N- and E-cadherins,<sup>11</sup> DAPT may not specifically act on Notch and may target other signaling molecules. We used a local RNA interference technique to confirm the effect of Notch on neuropathic pain, and shRNA-Notch1 and shRNA-control were microinjected into the ACC before the CCI surgery (Figs. 4A and B). Western blot result showed a significant reduction in NICD levels in the ACC 3 weeks after the microinjection of shRNA-Notch1 (Fig. 4C, CCI + shRNA-control vs CCI + shRNA-Notch1,  $P = 0.0014$ , Student  $t$ -test,  $n = 8$ ). At 21 days after microinjections of AAV-Notch1 and AAV-control, GFP expression was detected in the coronal section through the ACC (Fig. 4D). It showed that microinjection of AAV-control had no effect on pain perception of CCI rats; the paw withdrawal threshold and the paw withdrawal latency were significantly attenuated in CCI group and had no obvious changes in sham group by Notch1 interference (Figs. 4E and F). Moreover, the microinjection of shRNA-Notch1 did not change the total and center distance traveled or the total and center travel time during the 30-min recording time in the open-

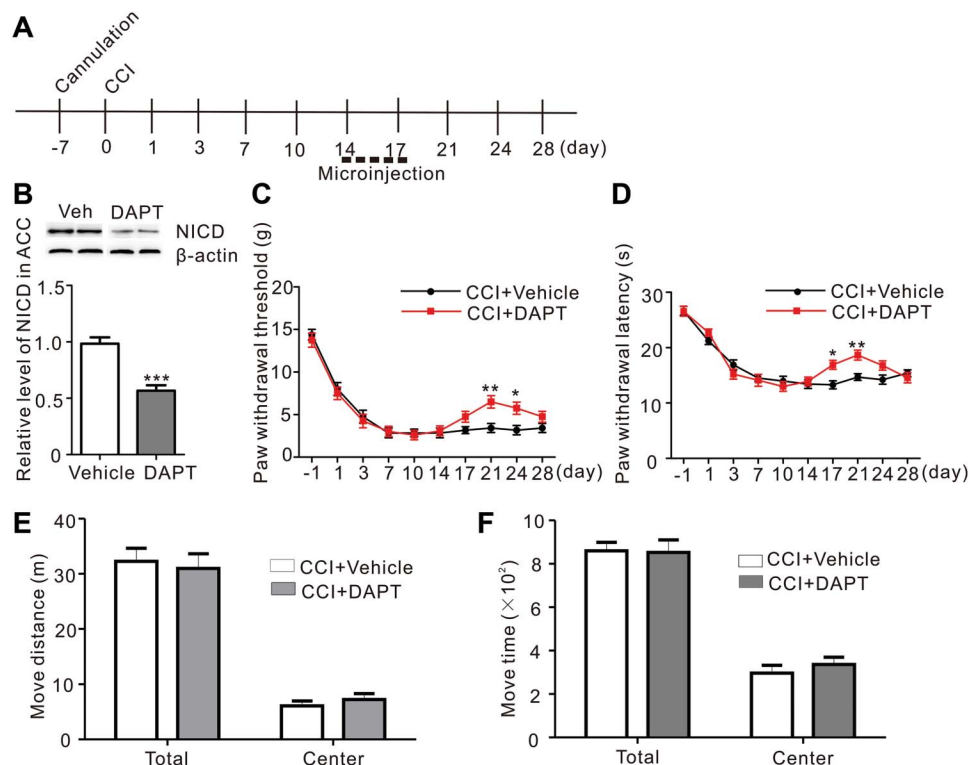


**Figure 3.** Microinjections of DAPT into the ACC 2 weeks after CCI relieved neuropathic for a few days and had no effect on the motor function. (A) Schematic of the late ACC microinjection experiments. (B) Seven days after the first microinjection, NICD levels were significantly decreased after the microinjection of DAPT compared to the Vehicle ( $P < 0.001^{***}$ , Student  $t$ -test,  $n = 8$  animals per group). (C) The microinjection of DAPT into the ACC 14 days after CCI only reversed the mechanical allodynia for a few days ( $F = 2.218$ ,  $P = 0.0242^*$ ,  $n = 8$  animals per group, two-way ANOVA followed by the Bonferroni post hoc test, black: CCI + Vehicle, red: CCI + DAPT). (D) The DAPT microinjection administrated 14 days after CCI to ACC increased paw the withdrawal latency, but only for a few days ( $F = 2.988$ ,  $P = 0.0028^*$ ,  $n = 8$  animals per group, two-way ANOVA followed by the Bonferroni post hoc test, black: CCI + Vehicle, red: CCI + DAPT). (E) Microinjections into ACC for 5 consecutive days did not affect the total and center distance traveled during the 30-min recording time in the open-field test ( $n = 8$  animals per group). (F) Microinjections into ACC for 5 consecutive days did not affect the total and center travel time during the 30-minute recording time in the open-field test ( $n = 8$  animals per group). ACC, anterior cingulate cortex; ANOVA, analysis of variance; CCI, chronic constriction injury; DAPT, N-[N-(3,5-difluorophenacetyl)-l-alanyl]-S-phenylglycine t-butyl ester; NICD, Notch intracellular domain.

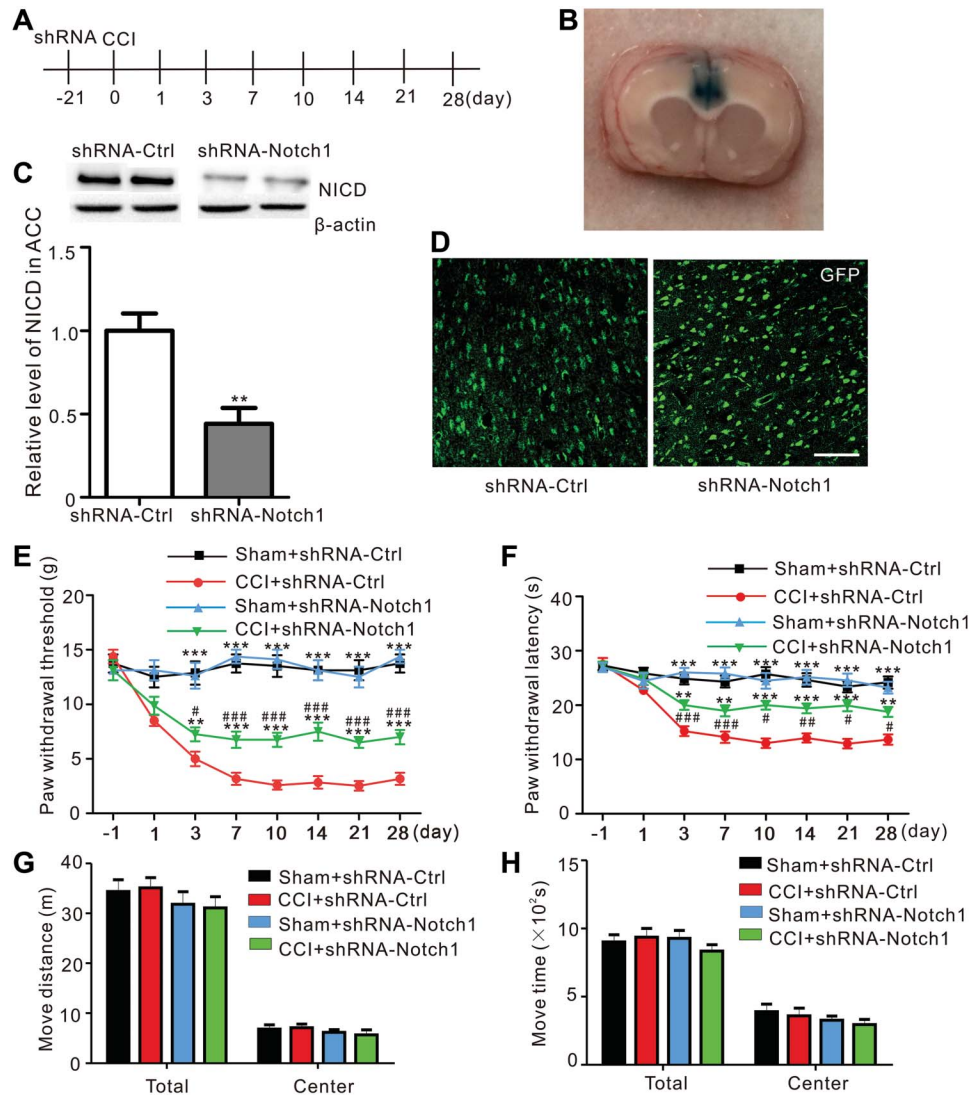


**Figure 4.** Microinjection of AAV-Notch1 into the ACC alleviated established CCI-induced mechanical allodynia and thermal hyperalgesia in rats. (A) Schematic of the pain behavior test and microinjection experiments. (B) The image shows an example of the location of microinjection site in one ACC slice. (C) Western blots of shRNA-Ctrl-infected and shRNA-Notch1-infected ACC with antibodies against NICD and  $\beta$ -actin. The levels of the NICD protein were quantified and normalized to  $\beta$ -actin ( $P = 0.0014^{**}$ , Student *t*-test,  $n = 8$  samples per group). (D) GFP expression was observed 21 days after the intra-ACC microinjections of AAV-Ctrl or AAV-Notch1. Scale bar 100  $\mu$ m. (E) Intra-ACC microinjections of AAV-Notch1, but not AAV-Ctrl, significantly partly reduced CCI-induced mechanical allodynia and had no effect on sham rats ( $F = 7.296$ ,  $P < 0.0001^{***}$ ,  $n = 8$  animals per group, two-way ANOVA followed by the Bonferroni post hoc test, \*: CCI + shRNA-Ctrl compared to CCI + shRNA-Notch1 and Sham + shRNA-Ctrl, #: CCI + shRNA-Ctrl compared to CCI + shRNA-Notch1; black: Sham + shRNA-Ctrl, red: CCI + shRNA-Ctrl, green: CCI + shRNA-Notch1, blue: Sham + shRNA-Notch1). (F) Attenuation of CCI-induced thermal hyperalgesia by shRNA-Notch1 ( $F = 4.940$ ,  $P < 0.0001^{***}$ ,  $n = 8$  animals per group, two-way ANOVA followed by the Bonferroni post hoc test, \*: CCI + shRNA-Ctrl compared to CCI + shRNA-Notch1 and Sham + shRNA-Ctrl, #: CCI + shRNA-Notch1 compared to Sham + shRNA-Notch1; black: Sham + shRNA-Ctrl, red: CCI + shRNA-Ctrl, green: CCI + shRNA-Notch1, blue: Sham + shRNA-Notch1). (G) Microinjections of the shRNA into the ACC did not affect the total and center distance traveled during the 30-min recording time in the open-field test ( $n = 8$  animals per group, black: Sham + shRNA-Ctrl, red: CCI + shRNA-Ctrl, green: CCI + shRNA-Notch1, blue: Sham + shRNA-Notch1). (H) Microinjections of AAV into the ACC did not affect the total and center travel time during the open-field test ( $n = 8$  animals per group, black: Sham + shRNA-Ctrl, red: CCI + shRNA-Ctrl, green: CCI + shRNA-Notch1, blue: Sham + shRNA-Notch1). AAV, adeno-associated virus; ACC, anterior cingulate cortex; ANOVA, analysis of variance; CCI, chronic constriction injury; GFP, green fluorescent protein; NICD, Notch intracellular domain; shRNA, short hairpin RNA.

field test (Figs. 4G and H). Thus, the downregulation of Notch1 in the ACC attenuated the development of neuropathic pain.

### 3.4. Disruption of Notch1 expression decreases synaptic transmission in the anterior cingulate cortex

An increase in excitatory synaptic transmission in the ACC is responsible for neuropathic pain generation.<sup>26</sup> We investigated the probability of  $\alpha$ -amino-3-hydroxy-5-methyl-4-isoxazole-propionic acid (AMPA) receptor-mediated responses of ACC

pyramidal neurons to verify that Notch1 contributes to the synaptic transmission potentiation in the ACC after nerve injury (Fig. 5A). The results were consistent with previous studies<sup>26,39</sup> because significant increases in the amplitude and frequency of mEPSCs were observed in the ACC neurons after CCI (days 7–14). Meanwhile, the amplitude and frequency of mEPSCs were significantly decreased in the shRNA-Notch1 group (Figs. 5B–E). Based on these results, Notch1 RNA interference in the ACC reversed the potentiation of synaptic transmission after peripheral nerve injury.

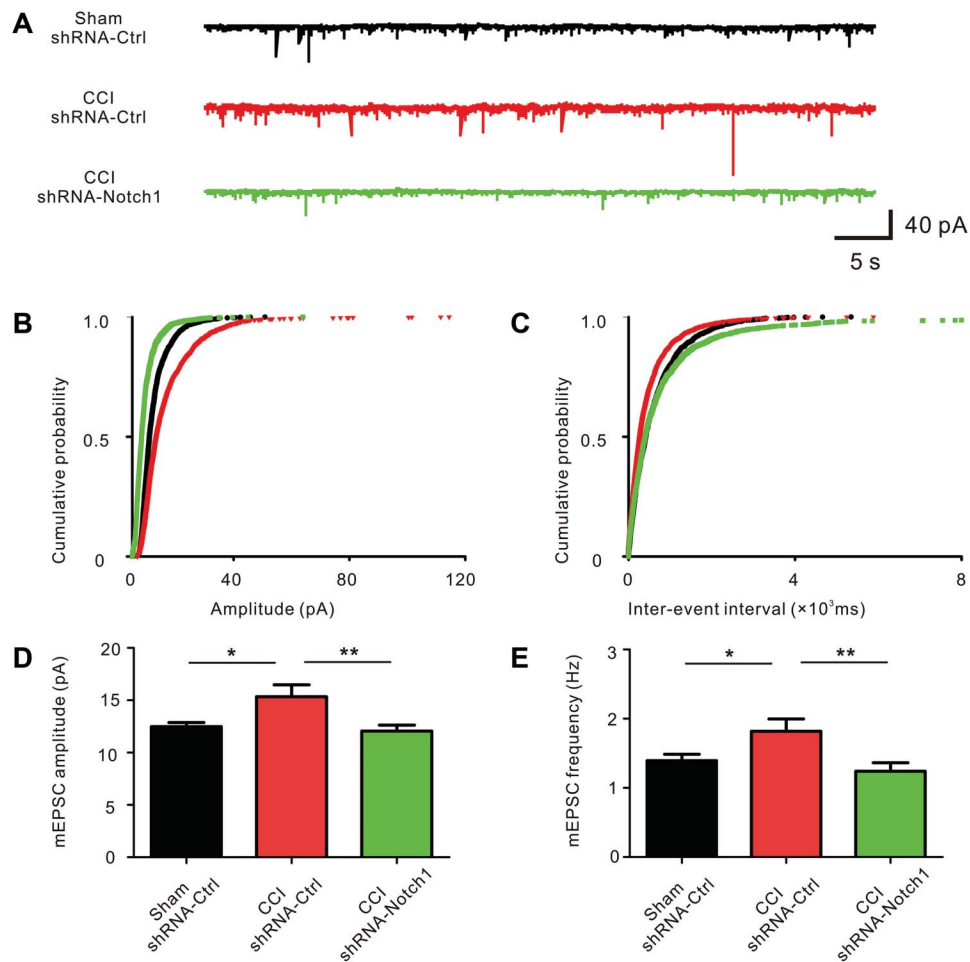


**Figure 5.** shRNA-Notch1 reversed the potentiation of synaptic transmission in the ACC. (A) Representative voltage clamp traces show mEPSCs recorded from ACC neurons in slices from different groups at a holding potential of  $-70$  mV. Scale bars represent 10 pA and 500 ms. (B) Cumulative probability representing the amplitude of mEPSCs in ACC neurons from different groups (black: Sham + shRNA-Ctrl, red: CCI + shRNA-Ctrl, green: CCI + shRNA-Notch1). (C) The cumulative probability represents the frequency of mEPSCs in ACC slices from different groups (black: Sham + shRNA-Ctrl, red: CCI + shRNA-Ctrl, green: CCI + shRNA-Notch1). (D) Amplitude of mEPSCs recorded in slices from Sham rats (black:  $n = 20$  neurons from 5 rats), rats after CCI (red:  $n = 18$  neurons from 5 rats), and shRNA-Notch1 group (green:  $n = 23$  neurons from 6 rats).  $*P < 0.05$ ,  $**P < 0.01$  compared with the CCI group. (E) Frequency of mEPSCs recorded in slices from Sham rats, rats after CCI, and rats after CCI with the shRNA-Notch1 microinjection.  $*P < 0.05$  and  $**P < 0.01$  compared with the CCI group. ACC, anterior cingulate cortex; CCI, chronic constriction injury; mEPSC, miniature excitatory postsynaptic current; shRNA, short hairpin RNA.

### 3.5. Downregulation of Hes1 attenuated neuropathic pain

The Hes family are effectors of Notch signaling that play a pivotal role in synaptic plasticity.<sup>27</sup> Hes1 and Hes5 are downstream effectors of the Notch signaling pathway.<sup>17</sup> The upregulation of the Notch1 mRNA was accompanied by an increase in the expression of the Hes1 mRNA, but not the Hes5 mRNA ([Fig. 6A, sham vs CCI,  $P = 0.0232$ , Student  $t$ -test]; [Fig. 6B, sham vs CCI,  $P = 0.0063$ , Student  $t$ -test]; [Fig. 6C, sham vs CCI,  $P = 0.7783$ , Student  $t$ -test],  $n = 6$ ). We established AAV vector systems to infect neurons with shRNA-Hes1 and shRNA-Hes5 (Fig. 6D). Hes1 expression was significantly reduced in the ACC after the AAV microinjection (Fig. 6E, CCI + shRNA-control vs CCI + shRNA-Hes1,  $P < 0.0001$ , Student  $t$ -test,  $n = 6$ ). In addition, the paw withdrawal threshold and the paw withdrawal latency were significantly attenuated by Hes1 downregulation in CCI-treated rats (Figs. 6F and G). Although Hes5 expression was significantly reduced in the ACC after the AAV microinjection as well, the pain behavior was not affected by Hes5 downregulation ([Fig. 6H, CCI + shRNA-control vs CCI + shRNA-Hes5,  $P < 0.0001$ , Student  $t$ -test,  $n = 6$ ], Figs 6I and J).

Therefore, Hes1, but not Hes5, played a key role in the pathological process of neuropathic pain.

### 3.6. Disruption of Notch1 reversed the mechanical allodynia in the spared nerve injury-induced neuropathic pain model

We wanted to determine whether increased NICD levels would be observed in other neuropathic pain models. An SNI model was successfully established (Figs. 7A and B), and NICD levels were significantly increased in the ACC of the SNI model 7 days after surgery, similar to the CCI model (Fig. 7C, sham vs SNI,  $P = 0.0282$ , Student  $t$ -test,  $n = 8$ ). Moreover, shRNA-Notch1 attenuated the mechanical allodynia in the SNI model as well (Fig. 7D). Thus, the activation of the Notch1 signaling pathway in the ACC is a general phenomenon induced by neuropathic pain.

## 4. Discussion

Peripheral nerve injury often results in central sensitization in the spinal cord, and supraspinal and cortical areas of the brain, including the somatosensory cortices, the amygdala, the

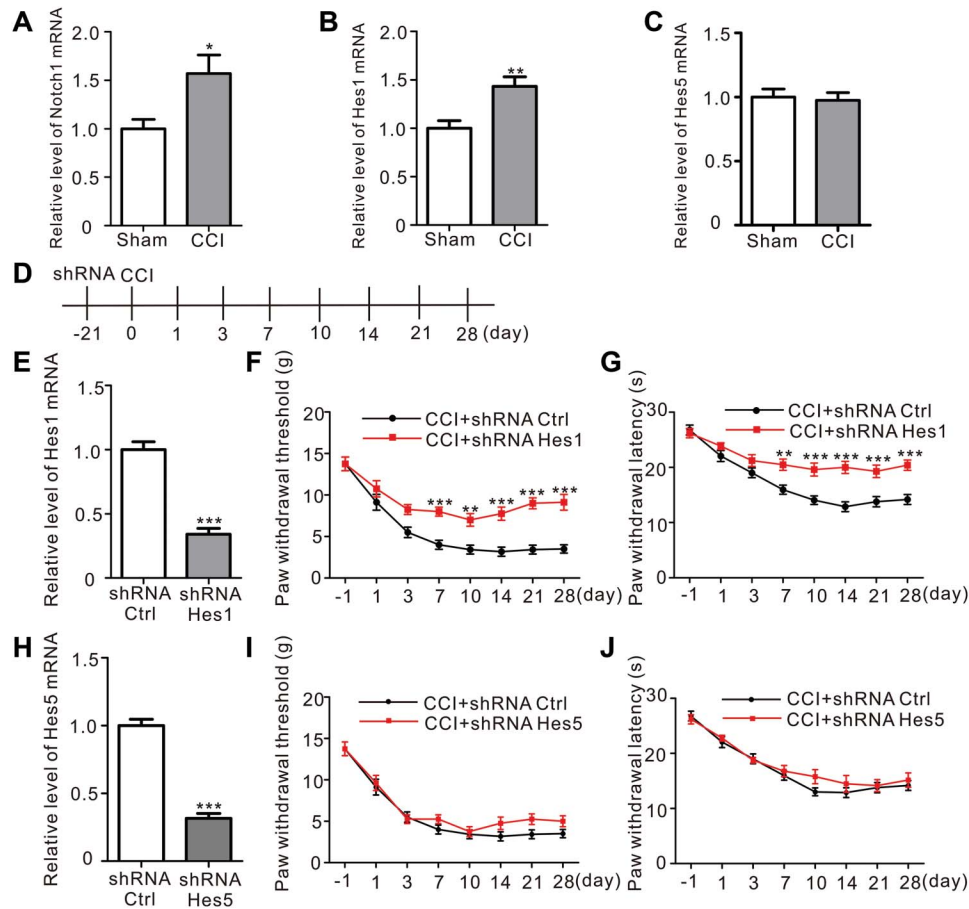


**Figure 6.** Hes1, but not Hes5, played an important role during CCI-induced neuropathic pain. (A) Levels of the Notch1 mRNA level of Notch1 in the CCI and Sham groups ( $P = 0.0232^*$ , Student  $t$ -test,  $n = 6$  samples per group). (B) The level of the Hes1 mRNA was significantly increased in the CCI group compared to the Sham group ( $P = 0.0063^{**}$ , Student  $t$ -test,  $n = 6$  samples per group). (C) The relative levels of the Hes5 mRNA in the CCI and Sham group ( $P = 0.7783$ , Student  $t$ -test,  $n = 6$  samples per group). (D) Schematic of ACC microinjections and behavior experiments. (E) Microinjection of shRNA-Hes1 into the ACC significantly decreased the level of the Hes1 mRNA detected using quantitative RT-PCR 21 days after the injection ( $P < 0.0001^{***}$ , Student  $t$ -test,  $n = 6$  samples per group). (F) Intra-ACC microinjections of shRNA-Hes1, but not shRNA-Ctrl, significantly reduced CCI-induced mechanical allodynia ( $F = 3.704$ ,  $P < 0.0012^{**}$ ,  $n = 8$  animals per group, two-way ANOVA followed by the Bonferroni post hoc test, black: CCI + shRNA-Ctrl, red: CCI + shRNA-Hes1). (G) Attenuation of CCI-induced thermal hyperalgesia by shRNA-Hes1 ( $F = 3.913$ ,  $P < 0.0007^{***}$ ,  $n = 8$  animals per group, two-way ANOVA followed by the Bonferroni post hoc test, black: CCI + shRNA-Ctrl, red: CCI + shRNA-Hes1). (H) Microinjections of shRNA-Hes5 into the ACC decreased the level of the Hes5 mRNA detected using quantitative RT-PCR 21 days after injection ( $P < 0.0001^{***}$ , Student  $t$ -test,  $n = 6$  samples per group). (I) Intra-ACC microinjections of shRNA-Hes5 did not exert significant effects on CCI-induced mechanical allodynia, similar to the shRNA-Ctrl injection ( $F = 0.6939$ ,  $P < 0.6771$ ,  $n = 8$  animals per group, two-way ANOVA followed by the Bonferroni post hoc test, black: CCI + shRNA-Ctrl, red: CCI + shRNA-Hes1). (J) Microinjections of shRNA-Hes5 into the ACC did not affect the thermal hyperalgesia induced by CCI ( $F = 0.5837$ ,  $P = 0.7679$ ,  $n = 8$  animals per group, two-way ANOVA followed by the Bonferroni post hoc test, black: CCI + shRNA-Ctrl, red: CCI + shRNA-Hes1). ACC, anterior cingulate cortex; ANOVA, analysis of variance; CCI, chronic constriction injury; Hes, hairy and enhancer of split; shRNA, short hairpin RNA.

prefrontal cortex, the insular cortex, and the ACC.<sup>14,18,21</sup> Plastic changes in those areas might result in increased pain sensitivity.<sup>45</sup> Here, we focused on the ACC, a key cortical area that is not only involved in processing pain-related emotion but also plays a role in the transmission of pain sensation.<sup>9,31,42,44,46</sup> Previous studies mainly focused on the role of Notch pathway in the determination of cell fate. The results presented in this study confirm the relation between the activation of the Notch signaling pathway in the central nervous system and the induction and maintenance of neuropathic pain.

Several studies have reported an association between the Notch pathway and neuropathic pain formation in the spinal cord, but researchers had not determined whether this pathway exerted the same effect on nerve injury in the central nervous system. In this study, NICD levels were increased in the ACC of 2 neuropathic pain models (CCI and SNI) in the early phase (day 7). However, there was no changes of NICD levels in the hippocampus, indicating that

the Notch signaling pathway may be activated specifically in the ACC after peripheral nerve injury. Notch intracellular domain levels increase in rat sciatic nerves and the dorsal horn of the spinal cord after injury, and the level of NICD also peaked at day 7 and lasted for 14 days.<sup>20,37</sup> Chen et al. identified direct descending projections from the pyramidal neurons in the ACC to the dorsal horn of the spinal cord.<sup>8</sup> According to the results from different studies, ACC activation induces long-lasting facilitation of spinal nociception that might be related to persistent hyperalgesia.<sup>8</sup> However, whether acute changes of NICD level contributed to the persistent pain was unknown. A gamma-secretase (a key enzyme involved in the Notch signaling pathway) inhibitor, DAPT, was microinjected in a rat model of CCI-induced neuropathic pain before or after the appearance of pain sensitivity to investigate the role of Notch signaling in the ACC during the pathological process of neuropathic pain. Early inhibition of the Notch signaling pathway persistently attenuated pain perception in a dose-dependent

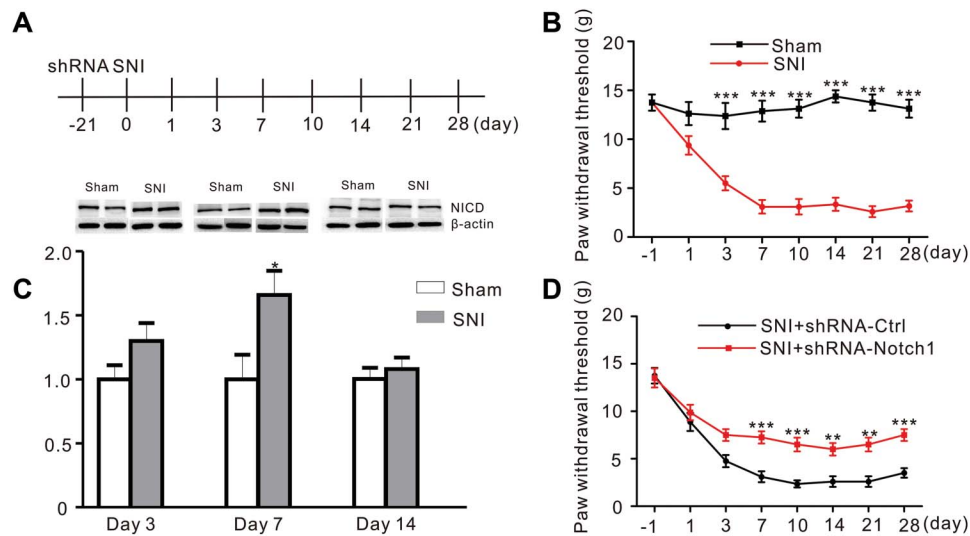


**Figure 7.** Microinjections of the Notch1 shRNA into the ACC inhibited mechanical allodynia induced by SNI in rats. (A) Schematic of ACC microinjections and behavior experiments. (B) Mechanical withdrawal thresholds were measured in Sham and SNI rats before and 1, 3, 7, 10, 14, 21, and 28 days after surgery. Results are presented as mean  $\pm$  SME ( $F = 11.19$ ,  $P < 0.0001^{***}$ ,  $n = 8$  animals per group, two-way ANOVA followed by the Bonferroni post hoc test, black: Sham, red: SNI). (C) Western blot showing increased NICD levels in the ACC (day 7 after surgery) in the SNI group and had no difference compared to Sham group at day 3 and 14. Bottom panel, quantification of the intensity of the NICD bands ( $P = 0.0282$ , Student  $t$ -test,  $n = 8$  animals per group). (D) Attenuation of SNI-induced mechanical allodynia by microinjections of shRNA-Notch1 into the ACC ( $F = 2.831$ ,  $P = 0.0094$ ,  $n = 8$  animals per group, two-way ANOVA followed by the Bonferroni post hoc test, black: SNI + shRNA-Ctrl, red: SNI + shRNA-Notch1). ACC, anterior cingulate cortex; ANOVA, analysis of variance; NICD, Notch intracellular domain; shRNA, short hairpin RNA; SNI, spared nerve injury.

manner. However, when DAPT was microinjected after neuropathic pain was established, it only ameliorated the behaviors for a short time. Combined with the increased levels of NICD observed on day 7 after CCI that recovered to the baseline values on day 14, we speculated that the Notch signaling pathway might have a prominent role in the early pathogenesis of neuropathic pain.

DAPT also participates in the proteolytic cleavage of deleted in colorectal cancer and amyloid precursor protein, in addition to Notch.<sup>11</sup> Because DAPT is a nonspecific inhibitor of Notch receptor, we then performed intra-ACC microinjections of an shRNA-Notch1-expressing recombinant AAV to validate the function of the Notch1 signaling pathway in neuropathic pain in the ACC. The silencing of Notch1 with an shRNA also significantly inhibited the development of neuropathic pain, similar to DAPT. The potentiation of synaptic transmission in the ACC was reported to be the key mechanism underlying neuropathic pain.<sup>8,9,48</sup> And a study showed that the activation of Notch signaling regulates synaptic transmission in the hippocampus.<sup>1</sup> Thus, given the possible link between synaptic transmission and the Notch signaling pathway in the pathological process of neuropathic pain, we further confirmed that the shRNA-Notch1-expressing recombinant AAV decreased excitatory synaptic transmission using electrophysiological techniques. Therefore, the increased NICD levels observed in the ACC after nerve injury might lead to the potentiation of synaptic transmission, and the subsequent generation of neuropathic pain after nerve injury.

The Notch signaling pathway controls the choice between excitatory and inhibitory cell fates during development, and its activation promotes the generation of excitatory neurons from the sensory interneuron progenitors.<sup>29</sup> Although we targeted neurons, the Notch1-expressing AAV vector mentioned above was nonselective because it did not use specific promoters to target certain populations of neurons, such as excitatory or inhibitory neurons. GABAergic disinhibition is considered a major mechanism of neuropathic pain.<sup>4,13</sup> Previous studies

have described links between the balance of glutamate/GABA transmission in the ACC and nociceptive responses, based on the hypothesis that GABAergic disinhibition may facilitate glutamate-mediated excitatory transmission in the ACC.<sup>30,42</sup> Thus, the mechanism by which the Notch signaling pathway regulates the balance of glutamate/GABA transmission during neuropathic pain requires further study. A recent study indicated a role for the Notch pathway in astrocyte activation after spinal cord injury.<sup>34</sup> Activation of glial cells is emerging as key mechanism underlying chronic pain.<sup>22,43</sup> Given the importance of supraspinal glial activation in the descending facilitation of nociception,<sup>43</sup> studies aiming to explore whether Notch signaling in glia also contributes to hypersensitivity in the ACC will be interesting.

The Hes family of transcription factors regulates neuronal function and morphology.<sup>17</sup> The human Hes family contains 7 members, Hes1-7, which are expressed in many tissues and play various roles mainly in development. These proteins may act alone or together to regulate different physiological and pathological processes.<sup>2,16,35</sup> Hes1 and Hes5 are downstream effectors of the canonical Notch signaling pathway, which regulates cell differentiation through cell-cell interactions.<sup>24</sup> In our study, we observed different changes in the pattern of expression of the Hes1 and Hes5 mRNAs under the condition of neuropathic pain. Seven days after CCI surgery, the expression of the Hes1 mRNA was significantly increased, whereas the expression of the Hes5 mRNA remained stable. Furthermore, the regulation of Hes1 expression exerted a significant effect on neuropathic pain behaviors, whereas Hes5 silencing did not. Thus, the Notch/Hes1 pathway may play a major role in the development of neuropathic pain.

In conclusion, the activation of the Notch/Hes1 signaling pathway was shown to potentially contribute to the potentiation of excitatory synaptic transmission in this study, which may lead to persistent pain after peripheral nerve injury.

## Conflict of interest statement

The authors have no conflicts of interest to declare.

## Acknowledgements

This work was supported by National Natural Science Foundation, Beijing, People's Republic of China (81671058 and 81730031 to Y. Wang); the Foundation of Shanghai Municipal Key Clinical Specialty (shslczdzk06901 to Y. Wang); and the Foundation of Shanghai Municipal Science and Technology Commission (19ZR1407500 to F. Shen).

Author contributions: Y. Wang, W. Liang, H. Duan, and F. Shen: established research concept and experimental design; H. Duan, L. Li, Z. Tu, F. Shen, and P. Chen: performed research and obtained the data; H. Duan, L. Li, F. Shen, and P. Chen: performed data analysis and interpretation of data; H. Duan, F. Shen, W. Liang, and Y. Wang: wrote the manuscript. Y. Wang and F. Shen: obtained funding; Z. Wang: provided technical and material support.

## Article history:

Received 9 February 2020

Received in revised form 1 July 2020

Accepted 13 July 2020

Available online 21 July 2020

## References

- Alberi L, Liu S, Wang Y, Badie R, Smith-Hicks C, Wu J, Pierfelice TJ, Abazyan B, Mattson MP, Kuhl D, Pletnikov M, Worley PF, Gaiano N. Activity-induced Notch signaling in neurons requires Arc/Arg3.1 and is essential for synaptic plasticity in hippocampal networks. *Neuron* 2011; 69:437–44.
- Bansod S, Kageyama R, Ohtsuka T. Hes5 regulates the transition timing of neurogenesis and gliogenesis in mammalian neocortical development. *Development* 2017;144:3156–67.
- Bennett GJ, Xie YK. A peripheral mononeuropathy in rat that produces disorders of pain sensation like those seen in man. *PAIN* 1988;33: 87–107.
- Blom SM, Pfister JP, Santello M, Senn W, Nevian T. Nerve injury-induced neuropathic pain causes disinhibition of the anterior cingulate cortex. *J Neurosci* 2014;34:5754–64.
- Brai E, Marathe S, Astori S, Fredj NB, Perry E, Lamy C, Scotti A, Alberi L. Notch1 regulates hippocampal plasticity through interaction with the reelin pathway, glutamatergic transmission and CREB signaling. *Front Cell Neurosci* 2015;9:447.
- Campbell JN, Meyer RA. Mechanisms of neuropathic pain. *Neuron* 2006; 52:77–92.
- Chaplan SR, Bach FW, Pogrel JW, Chung JM, Yaksh TL. Quantitative assessment of tactile allodynia in the rat paw. *J Neurosci Methods* 1994; 53:55–63.
- Chen T, Taniguchi W, Chen QY, Tozaki-Saitoh H, Song Q, Liu RH, Koga K, Matsuda T, Kaito-Sugimura Y, Wang J, Li ZH, Lu YC, Inoue K, Tsuda M, Li YQ, Nakatsuka T, Zhuo M. Top-down descending facilitation of spinal sensory excitatory transmission from the anterior cingulate cortex. *Nat Commun* 2018;9:1886.
- Chen ZY, Shen FY, Jiang L, Zhao X, Shen XL, Zhong W, Liu S, Wang ZR, Wang YW. Attenuation of neuropathic pain by inhibiting electrical synapses in the anterior cingulate cortex. *Anesthesiology* 2016;124: 169–83.
- Craig AD, Serrano LP. Effects of systemic morphine on lamina I spinothalamic tract neurons in the cat. *Brain Res* 1994;636:233–44.
- Dash PK, Moore AN, Orsi SA. Blockade of gamma-secretase activity within the hippocampus enhances long-term memory. *Biochem Biophys Res Commun* 2005;338:777–82.
- Decosterd I, Woolf CJ. Spared nerve injury: an animal model of persistent peripheral neuropathic pain. *PAIN* 2000;87:149–58.
- Dedek A, Xu J, Kandedgedara CM, Lorenzo LE, Godin AG, De Koninck Y, Lombroso PJ, Tsai EC, Hildebrand ME. Loss of STEP61 couples disinhibition to N-methyl-d-aspartate receptor potentiation in rodent and human spinal pain processing. *Brain* 2019;142:1535–46.
- Guida F, Luongo L, Marmo F, Romano R, Iannotta M, Napolitano F, Belardo C, Marabese I, D'Aniello A, De Gregorio D, Rossi F, Piscitelli F, Lattanzi R, de Bartolomeis A, Ussiello A, Di Marzo V, de Novellis V, Maione S. Palmitoylethanolamide reduces pain-related behaviors and restores glutamatergic synapses homeostasis in the medial prefrontal cortex of neuropathic mice. *Mol Brain* 2015;8:47.
- Hargreaves K, Dubner R, Brown F, Flores C, Joris J. A new and sensitive method for measuring thermal nociception in cutaneous hyperalgesia. *PAIN* 1988;32:77–88.
- Huang H, Lai S, Luo Y, Wan Q, Wu Q, Wan L, Qi W, Liu J. Nutritional preconditioning of apigenin alleviates myocardial ischemia/reperfusion injury via the mitochondrial pathway mediated by notch1/hes1. *Oxid Med Cell Longev* 2019;2019:7973098.
- Iso T, Kedes L, Hamamori Y. HES and HERP families: multiple effectors of the Notch signaling pathway. *J Cell Physiol* 2003;194:237–55.
- Jaggi AS, Singh N. Role of different brain areas in peripheral nerve injury-induced neuropathic pain. *Brain Res* 2011;1381:187–201.
- Jensen TS, Baron R, Haanpaa M, Kalso E, Loeser JD, Rice AS, Treede RD. A new definition of neuropathic pain. *PAIN* 2011;152:2204–5.
- Jeon D, Kim S, Chetana M, Jo D, Ruley HE, Lin SY, Rabah D, Kinet JP, Shin HS. Observational fear learning involves affective pain system and Cav1.2 Ca<sup>2+</sup> channels in ACC. *Nat Neurosci* 2010;13:482–8.
- Ji G, Zhang W, Mahimainathan L, Narasimhan M, Kiritoshi T, Fan X, Wang J, Green TA, Neugebauer V. 5-HT<sub>2C</sub> receptor knockdown in the amygdala inhibits neuropathic-pain-related plasticity and behaviors. *J Neurosci* 2017;37:1378–93.
- Ji RR, Berta T, Nedergaard M. Glia and pain: is chronic pain a gliopathy? *PAIN* 2013;154(suppl 1):S10–28.
- Juarez-Salinas DL, Braz JM, Etlin A, Gee S, Sohal V, Basbaum AI. GABAergic cell transplants in the anterior cingulate cortex reduce neuropathic pain aversiveness. *Brain* 2019;142:2655–69.
- Kobayashi T, Kageyama R. Expression dynamics and functions of Hes factors in development and diseases. *Curr Top Dev Biol* 2014;110:263–83.
- Li J, Han Y, Li M, Nie C. Curcumin promotes proliferation of adult neural stem cells and the birth of neurons in alzheimer's disease mice via notch signaling pathway. *Cell Reprogram* 2019;21:152–61.
- Li XY, Ko HG, Chen T, Descalzi G, Koga K, Wang H, Kim SS, Shang Y, Kwak C, Park SW, Shim J, Lee K, Collingridge GL, Kaang BK, Zhuo M. Alleviating neuropathic pain hypersensitivity by inhibiting PKMzeta in the anterior cingulate cortex. *Science* 2010;330:1400–4.
- Lin CH, Lee EH. JNK1 inhibits GluR1 expression and GluR1-mediated calcium influx through phosphorylation and stabilization of Hes-1. *J Neurosci* 2012;32:1826–46.
- Lopez-Guerra M, Xargay-Torrent S, Fuentes P, Roldan J, Gonzalez-Farre B, Rosich L, Silkenstedt E, Garcia-Leon MJ, Lee-Verges E, Gimenez N, Giro A, Aymerich M, Villamor N, Delgado J, Lopez-Guillermo A, Puente XS, Campo E, Toribio ML, Colomer D. Specific NOTCH1 antibody targets DLL4-induced proliferation, migration, and angiogenesis in NOTCH1-mutated CLL cells. *Oncogene* 2020;39:1185–97.
- Mizuguchi R, Kriks S, Cordes R, Gossler A, Ma Q, Goulding M. Ascl1 and Gsh1/2 control inhibitory and excitatory cell fate in spinal sensory interneurons. *Nat Neurosci* 2006;9:770–8.
- Narita M, Niikura K, Nanjo-Niikura K, Narita M, Furuya M, Yamashita A, Saeki M, Matsushima Y, Imai S, Shimizu T, Asato M, Kuzumaki N, Okutsu D, Miyoshi K, Suzuki M, Tsukiyama Y, Konno M, Yomiya K, Matoba M, Suzuki T. Sleep disturbances in a neuropathic pain-like condition in the mouse are associated with altered GABAergic transmission in the cingulate cortex. *PAIN* 2011;152:1358–72.
- Park SI, Oh JH, Hwang YS, Kim SJ, Chang JW. Electrical stimulation of the anterior cingulate cortex in a rat neuropathic pain model. *Acta Neurochir Suppl* 2006;99:65–71.
- Pierfelice T, Alberi L, Gaiano N. Notch in the vertebrate nervous system: an old dog with new tricks. *Neuron* 2011;69:840–55.
- Price DD. Psychological and neural mechanisms of the affective dimension of pain. *Science* 2000;288:1769–72.
- Qian D, Li L, Rong Y, Liu W, Wang Q, Zhou Z, Gu C, Huang Y, Zhao X, Chen J, Fan J, Yin G. Blocking Notch signal pathway suppresses the activation of neurotoxic A1 astrocytes after spinal cord injury. *Cell Cycle* 2019;18:3010–29.
- Riesenberger AN, Conley KW, Le TT, Brown NL. Separate and coincident expression of Hes1 and Hes5 in the developing mouse eye. *Dev Dyn* 2018;247:212–21.
- Shi T, Apkarian AV. Morphology of thalamocortical neurons projecting to the primary somatosensory cortex and their relationship to spinothalamic terminals in the squirrel monkey. *J Comp Neurol* 1995;361:1–24.
- Sun YY, Li L, Liu XH, Gu N, Dong HL, Xiong L. The spinal notch signaling pathway plays a pivotal role in the development of neuropathic pain. *Mol Brain* 2012;5:23.

- [38] Torrance N, Smith BH, Bennett MI, Lee AJ. The epidemiology of chronic pain of predominantly neuropathic origin. Results from a general population survey. *J Pain* 2006;7:281–9.
- [39] Toyoda H, Zhao MG, Zhuo M. Enhanced quantal release of excitatory transmitter in anterior cingulate cortex of adult mice with chronic pain. *Mol Pain* 2009;5:4.
- [40] Tsuda M, Koga K, Chen T, Zhuo M. Neuronal and microglial mechanisms for neuropathic pain in the spinal dorsal horn and anterior cingulate cortex. *J Neurochem* 2017;141:486–98.
- [41] Veceli DSF, Fortini F, Aquila G, Campo G, Vaccarezza M, Rizzo P. Notch signaling regulates immune responses in atherosclerosis. *Front Immunol* 2019;10:1130.
- [42] Wang H, Ren WH, Zhang YQ, Zhao ZQ. GABAergic disinhibition facilitates polysynaptic excitatory transmission in rat anterior cingulate cortex. *Biochem Biophys Res Commun* 2005;338:1634–9.
- [43] Wei F, Guo W, Zou S, Ren K, Dubner R. Supraspinal glial-neuronal interactions contribute to descending pain facilitation. *J Neurosci* 2008;28:10482–95.
- [44] Weston CS. Another major function of the anterior cingulate cortex: the representation of requirements. *Neurosci Biobehav Rev* 2012;36:90–110.
- [45] Woolf CJ, Salter MW. Neuronal plasticity: increasing the gain in pain. *Science* 2000;288:1765–9.
- [46] Xie K, Qiao F, Sun Y, Wang G, Hou L. Notch signaling activation is critical to the development of neuropathic pain. *Bmc Anesthesiol* 2015;15:41.
- [47] Xu H, Wu LJ, Wang H, Zhang X, Vadakkan KI, Kim SS, Steenland HW, Zhuo M. Presynaptic and postsynaptic amplifications of neuropathic pain in the anterior cingulate cortex. *J Neurosci* 2008;28:7445–53.
- [48] Yang Z, Tan Q, Cheng D, Zhang L, Zhang J, Gu EW, Fang W, Lu X, Liu X. The changes of intrinsic excitability of pyramidal neurons in anterior cingulate cortex in neuropathic pain. *Front Cell Neurosci* 2018;12:436.